Deducing the Electron-Beam Diameter in a Laser-Plasma Accelerator Using X-Ray Betatron Radiation

Michael Schnell,[1] Alexander Sävert,[1] Björn Landgraf,[1,2] Maria Reuter,[1,2] Maria Nicolai,[1] Oliver Jäckel,[1,2] Christian Peth,[3] Tobias Thiele,[3] Oliver Jansen,[4] Alexander Pukhov,[4] Oswald Willi,[3] Malte C. Kaluza,[1,2] and Christian Spielmann[1,2]

[1]*Institut für Optik und Quantenelektronik, Friedrich-Schiller Universität Jena, Max-Wien-Platz 1, 07743 Jena, Germany*
[2]*Helmholtz-Institut Jena, Fröbelstieg 3, 07743 Jena, Germany*
[3]*Institut für Laser- und Plasmaphysik, Heinrich-Heine Universität Düsseldorf, 40225 Düsseldorf, Germany*
[4]*Institut für Theoretische Physik, Heinrich-Heine Universität Düsseldorf, 40225 Düsseldorf, Germany*
(Received 16 May 2011; published 13 February 2012; corrected 25 April 2012)

We investigate the properties of a laser-plasma electron accelerator as a bright source of keV x-ray radiation. During the interaction, the electrons undergo betatron oscillations and from the carefully measured x-ray spectrum the oscillation amplitude of the electrons can be deduced which decreases with increasing electron energies. From the oscillation amplitude and the independently measured x-ray source size of (1.8 ± 0.3) μm we are able to estimate the electron bunch diameter to be (1.6 ± 0.3) μm.

A pulsed, bright x-ray source in the spectral range up to a few kiloelectron volt (keV) is of great interest for temporally resolved x-ray spectroscopy in physics, material science, and biology. So far, this photon energy range was mainly covered by picosecond x-ray pulses from synchrotrons [1]. More recently, x-ray free-electron lasers increased the available peak brilliance by several orders of magnitude while reducing the pulse duration to a few ten femtoseconds [2,3]. Over the last few years, another promising approach towards a compact femtosecond x-ray source has been investigated, namely, betatron radiation emitted during laser-plasma interaction [4,5]. To realize such a betatron source, an ultraintense fs-laser pulse is focused into a gas jet. After the pulse's rising edge has fully ionized the gas the main part of the pulse interacts with a plasma. Electrons are expelled from the focal region by the laser pulse hence exciting a plasma wave in its wake. When this wave is driven so hard that it breaks electrons are injected into the associated electric field (the wake field) [6,7] by which they are accelerated in forward direction to energies in excess of 100 MeV. The transverse electric field together with an azimuthal magnetic field [8] lead to a transverse oscillation of the electrons emitting betatron radiation in the keV range. In the bubble regime, the motion is described by the characteristic betatron wavelength $\lambda_b = \lambda_p \sqrt{2\gamma} \propto \sqrt{1/n_e}$ [9]. Here, $\lambda_p = 2\pi c \sqrt{\varepsilon_0 m_e / n_e e^2}$ is the plasma wavelength, c the speed of light in vacuum, ϵ_0 the vacuum permittivity, m_e the electron's rest mass, n_e the plasma density, γ the relativistic Lorentz factor, and e the elementary charge. Highly relativistic electrons oscillate with the amplitude r_b leading to the emission of radiation confined to a cone with a half-opening angle $\theta = K/\gamma$, where K is the strength parameter of the plasma wiggler given by $K = 1.33 \times 10^{-10} \sqrt{\gamma (n_e/\mathrm{cm}^{-3})}(r_b/\mu\mathrm{m})$ [10]. For laser-plasma based betatron sources a value of $K \gg 1$ is typically used and the continuous radiation can be described by [9]

$$\frac{d^2 I}{dE d\Omega}\bigg|_{\theta=0} \simeq N \frac{3e^2}{2\pi^3 \hbar c \varepsilon_0} \gamma^2 \left(\frac{E}{E_{\mathrm{crit}}}\right)^2 K_{2/3}^2\left(\frac{E}{E_{\mathrm{crit}}}\right). \quad (1)$$

Here, I is the spectral flux emitted on axis, $K_{2/3}(\xi)$ is the modified Bessel function of the second kind, N is the number of oscillations and $E_{\mathrm{crit}} \simeq 5 \times 10^{-24} \gamma^2 (n_e/\mathrm{cm}^{-3})(r_b/\mu\mathrm{m})$ keV is the critical energy [10]. The ultrashort x-ray pulses [11–13] are emitted over a wide spectral range with a peak brightness as high as 10^{22} photons per second per mrad^2 per mm^2 per 0.1% bandwidth [14]. The high brightness is mainly governed by the small transverse source size of a few μm, which is closely linked to the transverse diameter of the emitting electron bunch. The latter parameter, which has so far defied an accurate determination, is—together with the radiation source size—important for many applications, but a small value is also a clear indication for a well collimated electron beam.

In this Letter, we present a careful spatial characterization of a laser-plasma based betatron source in order to estimate the transverse diameter of the electron bunch in the plasma accelerator. Comparing the experimentally measured betatron radiation spectrum with theoretical predictions [15] allows for the deduction of the betatron oscillation amplitude r_b of a single electron. Finally, the diameter of the electron bunch is deduced from the measured x-ray source size and the calculated betatron oscillation amplitude.

The experiments were performed with the multi-TW Ti: sapphire laser system JETI in Jena, delivering 36 fs pulses with an energy of 650 mJ on target at a wavelength of 800 nm. The pulses were focused by an $f/20$ off-axis parabolic mirror into the leading edge of a pulsed

supersonic He-gas jet formed by a conically shaped nozzle with a diameter of 3 mm. Having a focal spot-diameter of 19 μm at full-width at half-maximum (FWHM) an intensity of 1.9×10^{18} W/cm^2 was reached corresponding to an amplitude of the normalized vector potential $a_0 = 1.0$. The laser-accelerated electrons were analyzed with a magnetic dipol spectrometer having two separate scintillating screens optimized for detecting electrons in the range from 10–55 MeV and 60–240 MeV, respectively. The x-ray radiation was detected with a thermoelectrically cooled, back-illuminated x-ray CCD camera (ANDOR DO-936N-MOW-BN). The residual laser light and the low energy x-ray radiation (below 1 keV) were blocked by a permanent 50 μm Be-filter in front of the CCD. Furthermore, filters were added to ensure that less than one x-ray photon hit a single pixel on the CCD chip. In this operation mode the camera works as an energy sensitive x-ray spectrometer with an energy resolution better than 100 eV over the whole spectral range. For a reliable measurement we ruled out multiple x-ray hits on single or adjacent pixels and considered only single pixel absorption events.

The plasma density distribution was monitored using a Nomarski-type interferometer [16]. Back-lighting the plasma from the side with a synchronized laser pulse enabled us to follow the plasma evolution with a temporal resolution of $\sim$100 fs. Additionally, we fully characterized the neutral gas density distribution of the jet with a tomographic approach before the experiment [17]. With this experimental setup it was possible to simultaneously measure all important parameters determining the properties of the betatron radiation source, namely, the electron energy, the x-ray spectrum, and the plasma density for each laser shot.

For most of the experiments the laser was operated in a single-shot mode, but operation up to 0.5 Hz was possible, limited only by the read-out time of the detectors and the gas load in the vacuum chamber. Quasi-monoenergetic electron pulses were generated by varying the backing pressure and optimizing the laser focal spot position. Typical single-shot electron spectra are shown in Fig. 1

for slightly different plasma densities n_e between 1.8 and 2.2×10^{19} cm^{-3}. The spectra peak at energies of 67, 79, and 114 MeV with a FWHM between 1 MeV (a) and 3 MeV [(b) and (c)]. For an optimized electron source, showing a mononenergetic spectrum with high energy, we deduced the divergence of a single electron bunch to 3 mrad and 2.5 mrad in the direction of laser polarization (x axis) and perpendicular to it (y axis), respectively. Averaging over 30 consecutive shots we obtained a root-mean-square (r.m.s.) fluctuation of the electron-beam pointing of 17.2 and 12.5 mrad along the x and y axis, respectively.

An x-ray spectrum corresponding to the electron spectra in Fig. 1(b) is shown in Fig. 2. A 0.35 mm thick mylar filter cuts the spectrum for low photon energy and the decreasing quantum efficiency of the 18 μm thick silicon CCD chip [18] defines the high-energy detection limit. For a precise measurement of the betatron spectrum it was necessary to distinguish between the direct betatron radiation and background radiation generated, e.g., from electrons hitting the chamber walls. To distinguish between these two contributions a fraction of the direct x-ray beam was blocked by a 3 mm thick Pb-foil directly behind the electron spectrometer. Radiation detected in the shadow of this foil is background radiation and is subtracted from the measured signal. Taking into account the respective filter functions, the CCD quantum efficiency and the measured background signal we calculated the betatron spectrum from the measured single hit spectrum as shown in Fig. 2. For our experimental parameters the betatron spectrum emitted
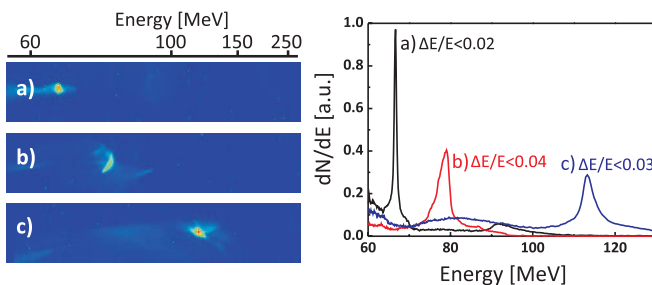

FIG. 1 (color). Three representative electron spectra with peaked features at (a) 67, (b) 79, and (c) 114 MeV. On the left we show raw data from the scintillator screen of the spectrometer and on the right the corresponding energy spectra together with the calculated energy spread.
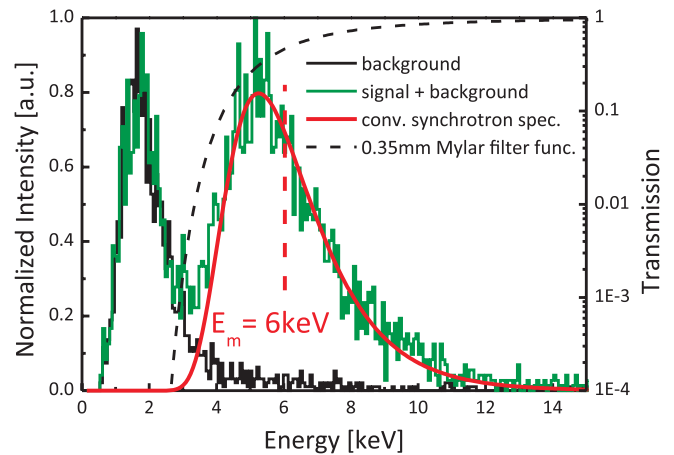

FIG. 2 (color). Normalized x-ray spectra in a range limited by the transmission of a 0.35 mm mylar filter for low photon energy and the reduced detection efficiency of the CCD for high photon energy. The black curve corresponds to the background, the green curve represents the sum of background and betatron radiation. Additionally, we show the transmission curve of a 0.35 mm thick mylar foil in front of the detector (dashed line). The red curve corresponds to the theoretically predicted spectrum convolved with the filter transmission and the CCD response for a betatron amplitude of $r_b = (0.9 \pm 0.3)$ μm.

by a single electron can be described by Eq. (1). The measured spectrum decreases exponentially in a range from 5–6 keV indicating a critical energy of $E_m = 6$ keV for the convoluted betatron spectrum. Now we can compare the measured single-shot spectrum with the theoretical model. Input parameters are the measured plasma density n_e and the peak-electron energy as well as the oscillation amplitude r_b as a free parameter. Note that for this evaluation we considered only strongly peaked electron spectra where the assumption of a narrow energy spread was justified. The theoretical spectrum [Eq. (1)] convolved with the filter functions and the spectral response of the CCD was fitted to the measured betatron signal and is shown in Fig. 2 (red curve). For the electron energy distribution of Fig. 1(b) and the corresponding betatron spectrum of Fig. 2 the best agreement was achieved for an oscillation amplitude of $r_b = (0.9 \pm 0.3)$ μm. By experimentally varying the peak energy (e.g., by changing the plasma density) of the electrons (and hence the γ factor) we could deduce the amplitude of the betatron oscillation as a function of γ as shown in Fig. 3(a) for single laser shots. A higher electron energy,
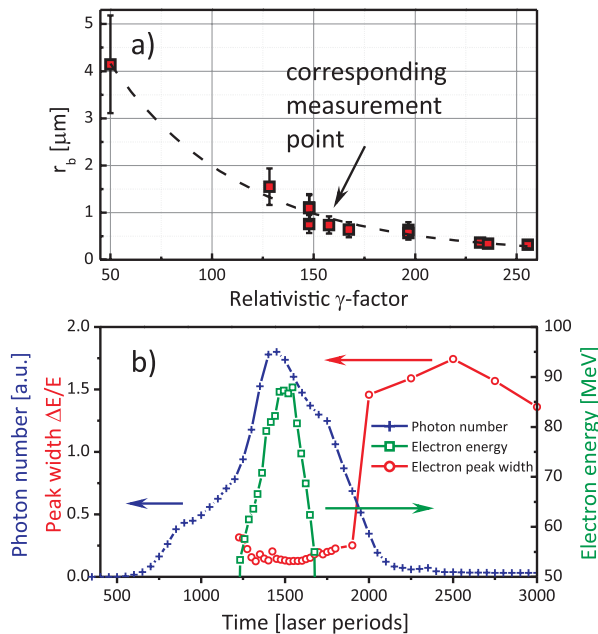
i.e., an increased electron mass γm_e, results in a smaller oscillation amplitude r_b. Since the theoretical treatment took into account single electrons only, the actual spot size of the x-ray beam produced by an electron bunch can be significantly larger.

To verify our experimental findings we performed a three-dimensional particle-in-cell simulation [19]. The most important results are summarized in Fig. 3(b). During the interaction the energy spectrum of the injected electrons evolves from an initially broad distribution to narrow peaks with increasing peak energy. Once laser depletion or dephasing between the electrons and the plasma wave sets in, the electron's peak energy is reduced again and the spectral shape becomes broader again [20]. The simulations also reveal that the largest number of keV photons is emitted from the region in the plasma where the electrons have the maximum energy at minimal spectral width. Since we only chose electron spectra showing a narrow energy spread for our further evaluation, these electrons obviously did not suffer from dephasing which lets us conclude that the major fraction of the experimentally detected betatron radiation from these interactions was mainly emitted from a region near the end of the plasma. Furthermore, the 3D PIC simulations confirmed the experimentally deduced value for the oscillation amplitude of the electron bunch of (1.5 ± 0.2) μm.

The electron bunch diameter can be obtained from the x-ray beam profile. Figure 4(a) shows the single-shot far field distribution of the betatron radiation measured 1.6 m behind the interaction for a monoenergetic electron beam. It has a nearly Gaussian distribution with a divergence of only 10 mrad.

FIG. 3 (color). (a) Experimentally measured betatron oscillation amplitude r_b as a function of the electron's γ factor. The dashed line is to guide the eye. The arrow indicates the data set mentioned in the text which was used for further evaluation. (b) 3D PIC simulation results showing the number of emitted photons per time interval (blue crosses), the peak-electron energy (green squares) and the relative width of the monoenergetic peak at the end of the electron spectrum (red circles) as a function of time in laser periods. As long as the electron bunch has a narrow energy spread at the maximum electron energy (only plotted above 50 MeV), i.e., before deceleration sets in (for $1250 < t < 1700$) the largest total number of photons is emitted.
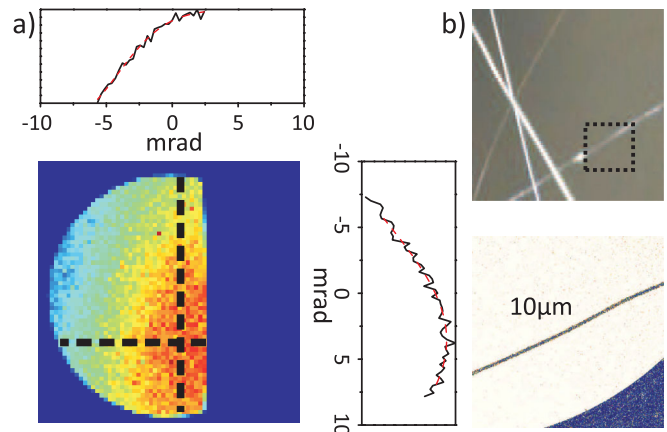

FIG. 4 (color). (a) Single-shot x-ray beam profile measured 1.6 m behind the gas jet. The right part of the beam is blocked to measure the background. The horizontal and vertical line-outs of the x-ray beam profile are fitted by a Gaussian distribution (red dashed curve) with an emission cone of 10 mrad. (b) Single-shot shadow image of thin tungsten wires having thicknesses between 10 and 40 μm (upper image). Shadow of a 10 μm wire only (lower image). The thinnest wire is still clearly visible indicating an x-ray source size smaller than the wire diameter.

For determining the electron bunch diameter we have estimated the x-ray spot size from a shadowgram. Tungsten wires with diameters of 10, 20, and 40 μm were placed behind the target in the beam path of the x rays. Figure 4(b) shows a single-shot shadowgram of a wire with 10 μm diameter. The wire is clearly visible, thus indicating a betatron source size smaller than the wire diameter. Fitting an error function to the shadowgram reveals a source size of $\sigma \leq 5$ μm which is in good agreement with previously reported numbers [14,21]. A closer inspection of the shadowgram reveals diffraction features which can be described by a Fresnel diffraction approach. Starting at the source plane we calculate the electric field at the 10 μm tungsten wire. The wire is described by its cylindrical shape, complex index of refraction, and a negligible surface roughness. Subsequently, we calculate the intensity distribution at the detector from the electric field modified by the wire. As the Fresnel theory is monochromatic, we simulate the intensity distribution at the detector for different photon energies considering the energy dependent refractive index of the wire. The monochromatic images were added after weighting in agreement with the measured (unfolded) spectra (see Fig. 2). According to the Fresnel diffraction theory the source intensity distribution is fully determined by the setup (distances, shape of the wire) and the spectrum. Thus, the accuracy of the retrieved source size is mainly limited by measurement errors of these quantities. Figure 5 shows a lineout of the measured intensity distribution (black squares) and a best-fit of the source size (green curve). The source size information is already encrypted within the first overshot at the edge of the wire's shadow. Assuming a Gaussian intensity distribution of the x-ray source, which is justified by the Gaussian-like beam profile in the far field [see Fig. 4(a)], the mentioned Fresnel diffraction modeling reveals an
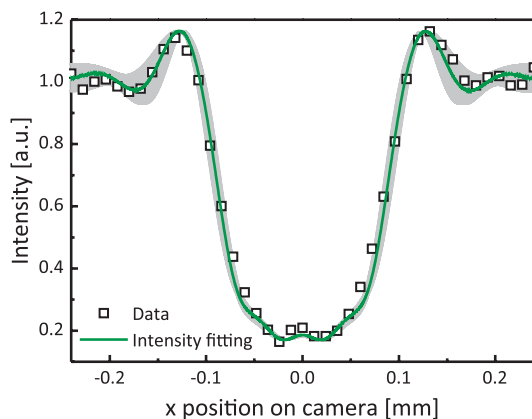

FIG. 5 (color). Measured (squares) and simulated (green) intensity distribution of a wire shadow on a detector using Fresnel diffraction for a radiation source with a broadband betatron spectrum ($E_m = 6$ keV) and a Gaussian shape for a source size of $\sigma = (1.8 \pm 0.3)$ μm. The gray area represents the error band of (± 0.3) μm.

upper limit for the radiation source size of (1.8 ± 0.3) μm FWHM only. This small spot size of the betatron radiation is very encouraging for applications requiring a high peak brightness x-ray source.

Finally, we determined the electron bunch diameter from the x-ray source size. For our experimental conditions we found a betatron oscillation wavelength of $\lambda_b = 125$ μm and according to Fig. 3(b) the radiation is mainly emitted in a few oscillations. In this range, the evolution of the betatron intensity distribution $I_b(\vec{r}, z)$ can be described by a propagation operator $P(z, r_b)$ and the electron distribution $\rho_{e^-}(\vec{r}, z)$. To retrieve the electron distribution the deconvolution of $\rho_{e^-}(\vec{r}, z) * P(z, r_b) \propto I_b(\vec{r}, z)$ has to be carried out with the help of inverse filtering. As both the propagation operator and the betatron field are Gaussian-like, the deconvolution will also yield a Gaussian-like electron distribution. Using this approach, we could estimate the FWHM radius of the electron bunch to (1.6 ± 0.3) μm inside the laser-plasma accelerator near the exit.

In conclusion, we have measured the spectrum of a betatron source in the keV range with a spectral resolution of less than 100 eV. The simultaneous measurement of the x-ray and electron spectra allowed a determination of the betatron oscillation amplitude r_b as a function of the electron energy. The obtained magnitude and scaling are in good agreement with recently published simulations [10,22]. From the oscillation amplitude and the independently measured x-ray source size of (1.8 ± 0.3) μm we could for the first time estimate the electron bunch radius (FWHM) to (1.6 ± 0.3) μm. The experimentally estimated number of 1×10^6 x-ray photons above 5 keV in each shot in combination with the spot size and the low divergence results in a peak brightness of 5×10^{21} photons per second per mrad^2 per mm per 0.1% bandwidth, using the laser pulse duration of 30 fs as an upper limit of the x-ray pulse duration. With this deduced peak brightness time-resolved x-ray absorption measurements become feasible.

[1] T. Pfeifer et al., Rep. Prog. Phys. **69**, 443 (2006).
[2] W. Ackermann et al., Nature Photon. **1**, 336 (2007).
[3] P. Emma et al., Nature Photon. **4**, 641 (2010).
[4] A. Rousse et al., Phys. Rev. Lett. **93**, 135005 (2004).
[5] K. T. Phuoc et al., Phys. Plasmas **12**, 023101 (2005).
[6] A. Modena et al., Nature (London) **377**, 606 (1995).
[7] K. Nakajima et al., Phys. Rev. Lett. **74**, 4428 (1995).
[8] M. C. Kaluza et al., Phys. Rev. Lett. **105**, 115002 (2010).
[9] E. Esarey et al., Phys. Rev. E **65**, 056505 (2002).
[10] F. Albert et al., Phys. Rev. E **77**, 056402 (2008).
[11] K. T. Phuoc et al., Phys. Plasmas **14**, 080701 (2007).

[12] O. Lundh *et al.*, Nature Phys. **7**, 219 (2011).

[13] A. Buck *et al.*, Nature Phys. **7**, 543 (2011).

[14] S. Kneip *et al.*, Nature Phys. **6**, 980 (2010).

[15] S. Fourmaux *et al.*, New J. Phys. **13**, 033017 (2011).

[16] R. Benattar *et al.*, Rev. Sci. Instrum. **50**, 1583 (1979).

[17] B. Landgraf *et al.*, Rev. Sci. Instrum. **82**, 083106 (2011).

[18] http://www.andor.com/scientific_cameras/x-ray/.

[19] A. Pukhov, J. Plasma Phys. **61**, 425 (1999).

[20] C. M. Huntington *et al.*, Phys. Rev. Lett. **106**, 105001 (2011).

[21] R. Shah *et al.*, Phys. Rev. E **74**, 045401 (2006).

[22] K. T. Phuoc *et al.*, Phys. Rev. Lett. **97**, 225002 (2006).